Biochimica et Biophysica Acta, 679 (1982) 353–360
Elsevier Biomedical Press

BBA 41027

CHLOROPHYLL *a* IN BILAYER MEMBRANES

I. THE THERMAL PHASE DIAGRAM WITH DISTEAROYLPHOSPHATIDYLCHOLINE *

KENNETH E. EIGENBERG **, WILLIAM R. CROASMUN and SUNNEY I. CHAN ***

Arthur Amos Noyes Laboratory of Chemical Physics, California Institute of Technology, Pasadena, CA 91125 (U.S.A.)

(Received July 10th, 1981)

Key words: Lipid bilayer; Differential thermal analysis; Chlorophyll-lipid interaction; Photosynthetic membrane model

Several groups have introduced chlorophyll *a* into artificial bilayer membranes in an attempt to develop a model system for studying the behavior of chlorophyll in the photosynthetic membrane. In order to investigate the organization of chlorophyll in these model systems, mixed bilayer systems containing chlorophyll *a* and distearoylphosphatidylcholine under conditions of excess water have been studied by differential thermal analysis. The resulting data suggest a phase diagram for this system consisting of a double eutectic with formation of a thermodynamic compound of defined stoichiometry between chlorophyll *a* and phospholipid at temperatures below the liquidus. The phase diagram may be simulated to obtain thermodynamic parameters characteristic of the compound phase. It is apparent that the organization and intermolecular interactions of chlorophyll in a bilayer membrane can vary widely depending on the temperature and composition of the system. In particular, phase separation can occur within the membrane over certain temperature ranges, resulting in an inhomogeneous system. Thus in interpreting the physical and spectroscopic properties of chlorophyll *a* in bilayer membranes, it is essential to consider the phase state of the membrane and the organization and environment of the chlorophyll in the particular phase.

Introduction

Several groups have reported the inclusion of small amounts of chlorophyll *a* into artificial multilamellar and vesicular bilayer membrane systems [1–12] in an attempt to develop useful models for studying energy transfer [1,2] and photo-induced electron transfer [3–5], and to model the photosynthetic membrane itself [4–8]. As a result of these efforts it has been demonstrated that chlorophyll are integrally incorporated into the bilayer with the porphyrin headgroup in the polar region of the membrane [9,10] and the nonpolar phytol group inserted in the hydrophobic core of the membrane [6] along with the lipid fatty acyl chains. Conflicting interpretations have been offered, however, regarding the precise lateral membrane organization of chlorophyll and lipid and the concomitant intermolecular interactions. A clear understanding of the organization of chlorophyll in these model systems is essential if they are to be used to their full advantage.

Tomkiewicz and Corker [3] concluded from absorption, circular dichroism and electron paramagnetic resonance studies that chlorophyll *a* in egg lecithin vesicles (0.02–0.10 mole fraction chlorophyll *a*) is present in monomeric form, in other words with no direct chlorophyll-chlorophyll interactions, both at room temperature (above the membrane phase transition) and also at lower temperatures. Oettmeier et al.

Abbreviations: DSPC, distearoylphosphatidylcholine; DPPC, dipalmitoylphosphatidylcholine.

* Contribution No. 6478 of the Department of Chemistry, California Institute of Technology.

** Present address: Monsanto, 800 North Lindberg, Mail Stop Q2B, St. Louis, MO 63166, U.S.A.

*** To whom reprint requests should be sent.

0005-2728/82/0000–0000/$02.75

[5,9] reached a similar conclusion for chlorophyll *a*/dipalmitoylphosphatidylcholine (DPPC) vesicles (0.033 mole fraction chlorophyll *a*) at and below room temperature (below the phase transition). Lee [11], however, interpreted the decrease in chlorophyll *a* fluorescence at temperatures below the thermal phase transition of chlorophyll *a*/DPPC multilayers in terms of segregation of chlorophyll *a* into nonfluorescent oligomers. This fluorescence change is reversible with temperature, and both Lee [11] and Colbow [7] have used this to monitor the phase transition of various membrane systems, although it was noted that the measured transition temperature is altered by changes in chlorophyll concentration.

In the present study we show that the lateral organization of chlorophyll *a* within a host phospholipid bilayer membrane depends on both temperature and composition, and can in fact vary widely depending upon the particular set of conditions chosen. This result suggests that in using the chlorophyll *a*/phospholipid bilayer as a model system it is essential to assess the phase state of the membrane and to consider its effects on the properties of the system in question.

Materials and Methods

Synthetic β-γ-distearoyl-L-α-phosphatidylcholine (DSPC) was obtained from Calbiochem. Its purity was checked by thin-layer chromatography on Whatman LK5DF analytical plates developed with chloroform/methanol/water (65 : 25 : 4). Since no impurities were found the DSPC was used without further purification.

Chlorophyll *a* was isolated from spinach extracts by the dioxane precipitation procedure of Iriyama et al. [13] and purified by chromatography on powdered sugar according to Strain et al. [14,15]. Particular care was taken in the chromatographic separation to exclude bands due to chlorophyll *a* alteration products which elute slightly ahead of authentic chlorophyll *a*. The final purity of the isolated product was determined from the optical absorption spectrum in diethyl ether. Molar extinction coefficients were determined from the absorption of a solution of chlorophyll *a* (approx. 1 mg weighed to 0.1 μg) in 100 ml fresh diethyl ether. Molar extinction coefficients found (literature values [15] in parentheses): ϵ_{660} = $11.0 \cdot 10^4$ ($11.2 \cdot 10^4$), $\epsilon_{428} = 8.56 \cdot 10^4$ ($8.63 \cdot 10^4$) indicate that the purity is over 98%. The ratios of the absorption bands correspond well with previously determined values (literature values [16] in parentheses): $\epsilon_{428}/\epsilon_{660} = 1.29$ (1.31), $\epsilon_{428}/\epsilon_{410} = 1.59$ (1.57).

Stock solutions of chlorophyll *a* and DSPC were prepared in fresh chloroform and mixed in the appropriate amounts to obtain the necessary mole fraction of the two components. The solution was evaporated to dryness under nitrogen and the solid mixture dried overnight under vacuum. To prepare samples for thermal analysis, 2 mg of the chlorophyll *a*/DSPC mixtures was finely divided and placed in 2-mm glass capillary tubes. Deionized water (5 μl) was added and the capillary sealed. The samples were then allowed to hydrate for at least 2 h at 70°C in order to form a multilamellar dispersion.

Differential thermal analysis was carried out on a DuPont 900 Differential Thermal Analyzer. The calibration of the instrument was checked by determining the transition temperature of pure DSPC multilayers prepared in exactly the same manner as the chlorophyll *a*/DSPC multilayers. The sample thermocouple was placed in the approximate center of the sample and referenced against a matched amount of water in an identical reference capillary. Both sample and reference were heated at a uniform rate of 6 K/min from 30 to 70°C. Following its return to 30°C the sample was allowed to equilibrate for at least 30 min prior to subsequent measurements to eliminate possible hysteresis effects. The measured transition temperatures were taken as the peak of the exotherm. According to the analysis of Smyth [17] this procedure is correct for a thermocouple measuring the temperature at the center of a cylindrical sample heated from the outside.

Results

Differential thermal analysis (DTA) was performed on hydrated chlorophyll *a*/DSPC multilayers in order to determine the thermal phase diagram of the bilayer system. Differential thermal analysis thermograms from 30 to 70°C were obtained in triplicate at 2 mol% intervals over the composition range 0–50 mol% chlorophyll *a*. Peak positions for each composition were measured at the temperature of maximum

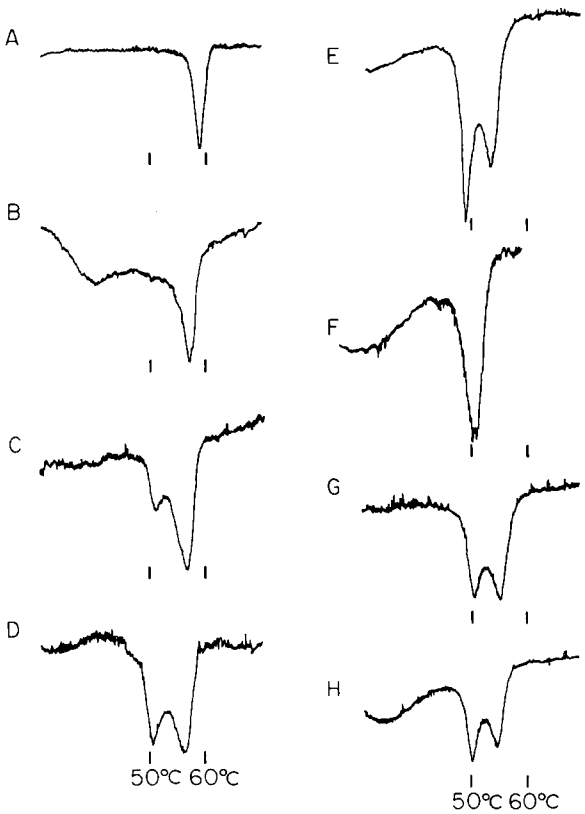

Fig. 1. Selected differential thermal analysis heating thermograms of hydrated chlorophyll *a*/DSPC multilayers (5 mg H_2O per 2 mg total lipid). Compositions (%): A, 2; B, 6; C, 8; D, 12; E, 22; F, 32; G, 40; H, 42.

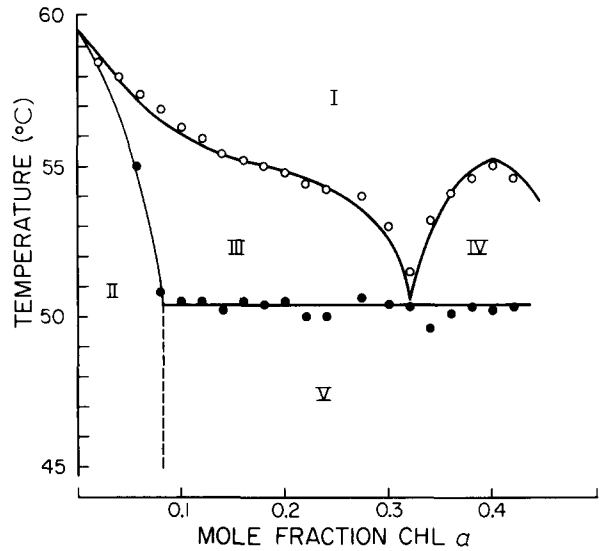

Fig. 2. Differential thermal analysis phase diagram of the chlorophyll *a*/DSPC bilayer membrane system prepared as an aqueous multilamellar suspension in excess water. Open and closed circles represent points of maximum exothermicity of the observed differential thermal analysis peaks. The liquidi between regions I and III, and between I and IV were calculated to fit the data as described in the text.

exothermicity and the triplicate values were averaged. The average standard deviation in the values was approx. 0.20°C.

Some typical thermograms at selected compositions are shown in Fig. 1. The changes in the number and positions of the observed exothermic peaks indicate that the number and identity of the phases present change over the temperature and composition range studied. Briefly, thermograms of compositions up to 6 mol% chlorophyll *a* show only a single unresolved peak that becomes broader with increasing chlorophyll *a* composition. At 6 mol% a small exotherm is partly resolved as a shoulder on the low-temperature side of the main peak. From 8 to 30 mol% chlorophyll *a*, two distinct exotherms are observed. The upper of these two decreases in temperature regularly with increasing chlorophyll *a* composition, while the lower maintains an average temperature of about 50°C. Near 32 mol% chlorophyll *a*, the previous two exotherms coalesce at what is apparently a eutectic point. Beyond 32 mol% two peaks again appear, the lower remaining near 50°C and the upper now increasing in temperature with increasing chlorophyll *a* content. At 42 mol% there is a slight but significant decrease in the temperature of the upper exotherm. Beyond 42 mol% the temperatures of the peaks no longer change and the sensitivity of the thermograms decreases, most likely indicating that the bilayer is saturated with chorophyll *a* at 42 mol%.

The transition temperatures for the various compositions are plotted to yield the two-component phase diagram shown in Fig. 2. The third component of the system, water, is present in large excess and we assume that its activity remains essentially unchanged in these experiments.

Discussion

Interpretation of the phase diagram

The pattern of the data in Fig. 2 suggests a particu-

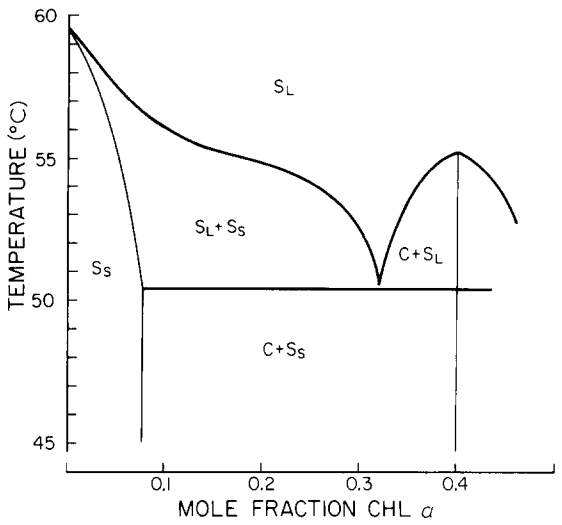

Fig. 3. Phase diagram of chlorophyll *a*/DSPC bilayers interpreted as a compound type of phase diagram with double side-by-side eutectics. Note that only a portion of the double eutectic phase diagram is observed in this system because of limited bilayer stability beyound about 42 mol% chlorophyll *a*. Abbreviations: S_L, liquid-crystalline bilayer solution. S_S, solid solution or limited miscibility region; C, compound phase – 0.40 mole fraction chlorophyll *a*.

lar form of phase diagram characteristic of compound formation between chlorophyll *a* and the phospholipid DSPC. The location and nomenclature of the various phases consistent with this interpretation of the phase diagram are shown in Fig. 3. Additional support for this interpretation as well as further characterization of some of the important phases is included in the following paper [24].

Several rules [18] aid in assignment of the phases present in each region of the temperature-composition space depicted in Fig. 2. (1) A two-component phase diagram must consist of unique one-phase and two-phase regions separated by lines of three-phase equilibria. (2) These regions must be arranged such that a horizontal isotherm alternately traverses one and two-phase regions. (3) A eutectic line is a line of three-phase equilibrium and must be a boundary for three two-phase regions, two above and one below it. The horizontal line in Fig. 2 at 50.4°C is clearly a eutectic line. Thus, rule 3 implies that regions III, IV and V should be two-phase regions in Fig. 2. Rule 2 then requires that regions I and II be one-phase regions. Finally, it follows that III and V must share a common phase. Likewise, IV and V must share a common phase.

In characterizing the phases, we first extrapolate from the phase behavior of pure DSPC (or zero chlorophyll) which has already been well documented. Above the main transition temperature of 59°C DSPC multilayers are in a fluid-like liquid crystalline phase. At lower temperatures DSPC multilayers exist in a more solid-like and ordered gel phase. Since regions I and II are continuous with these pure-component phase regions, it is expected that they should share similar features. Thus region I, which is a one-phase region, should consist of a fluid-like solution of chlorophyll *a* in the host DSPC bilayer. Similarly region II, also a homogeneous one-phase region, should consist of a solid solution of chlorophyll *a* in a gel phase with DSPC. To be sure, these are not solutions in the usual sense but must be considered as two-dimensional solutions within the bilayer plane. Region III, in equilibrium with the phases of regions I and II, must then consist of these two phases in relative amounts governed by the appropriate tie-line.

The data at higher chlorophyll *a* concentrations suggest two possible types of phase diagram, both involving partial solid state miscibility: (a) a two-component single-eutectic; or (b) compound formation with side-by-side eutectics. The actual phase diagram of the system must of course consist of only part of the complete phase diagram because the bilayer system breaks down at high chlorophyll compositions. In the case of phase diagram a, the two-phase region IV would consist of chlorophyll *a*/DSPC solution in equilibrium with a phase consisting of mostly chlorophyll *a* with a limited solubility of DSPC. The existence of such a phase seems quite unlikely, since chlorophyll does not form stable bilayers. Furthermore, the decrease in transition temperature at 42 mol% is inconsistent with a liquidus which should increase towards the right end composition. This decrease is, in fact, suggestive of the compound type of phase diagram shown in Fig. 3. We take this as evidence for compound formation between chlorophyll *a* and DSPC.

Simulation of the phase diagram

The experimental phase diagram of the chlorophyll *a*/DSPC bilayer system can be simulated to yield useful thermal parameters. For this analysis we

have adapted the treatment of Lee [19,20] for binary lipid mixtures, which takes into account nonideal mixing of the components. In the chlorophyll *a*/DSPC system, mixing is expected to be markedly nonideal because of the very different chemical structures and because of the necessary chemical interaction between chlorophyll *a* and the phospholipid to form the compound.

If chlorophyll *a* and the phospholipid form an ideal binary solution, the chemical potentials of the two components A and B, μ_A and μ_B, would be related to their relative mole fractions, X_A and X_B, in the solution by

$$\mu_A = \mu_A^\circ + RT \ln X_A \tag{1}$$

$$\mu_B = \mu_B^\circ + RT \ln X_B \tag{2}$$

The quantities μ_A° and μ_B° denote the standard-state chemical potentials of the two components. The assumption of an ideal solution is synonymous with a zero enthalpy of mixing. This requirement is rarely met by mixtures of lipid molecules because of intermolecular interactions. Furthermore, different molecular volumes can produce an additional entropy of mixing. These deviations from ideal behavior can be taken into account by introducing the activity coefficient, γ

$$\mu_A = \mu_A^\circ + RT \ln X_a \gamma_A, \tag{3}$$

or alternatively, the excess chemical potential μ^e.

$$\mu_A^e = RT \ln \gamma_A \tag{4}$$

Thus, because of nonideality, there is an excess molar Gibbs free energy of mixing for a binary mixture given by

$$\Delta G^e = X_A \mu_A^e + X_B \mu_B^e. \tag{5}$$

There has been some success [19,20] in modeling the excess Gibbs free energy for binary lipid mixtures using the approximate expression [21]:

$$\Delta G^e = X_A X_B \rho_0 \tag{6}$$

Here ρ_0 is a so-called nonideality parameter characteristic of differences in pair-wise interaction energies between nearest neighbors in the solution. It therefore contains information on the interaction energies between the two component species. Eqn. 6 does not explicitly take into consideration the excess free energy arising from different molecular volumes of the components lipids. However, for a binary mixture of chlorophyll *a* and DSPC, this contribution is likely to be small compared to the energy of mixing and we shall ignore it in the discussion to follow.

Deviations from ideality for a binary solution are reflected in the details of the liquidus phase boundaries of the phase diagram. For an ideal binary solution with complete immiscibility in the solid phase, the liquidus boundary is in fact just the well-known freezing point depression curve corresponding to the solubility of each solid component in the solution given by

$$\ln X_A^{liq} = \frac{\Delta H_A}{R}\left(\frac{1}{T_A} - \frac{1}{T_{ideal}}\right) \tag{7}$$

Here,. T_A and ΔH_A are the melting temperature and the heat of melting of the pure solid component A. Plotting T_{ideal} vs. X_A^{liq} yields the ideal liquidus boundary in this part of the phase diagram. The inclusion of nonideality would modify this liquidus. If the excess free energy of mixing is as formulated in Eqn. 6, then the transition temperature, T, expected for the nonideal mixture will deviate from the ideal solution temperature. T_{ideal}, approximately by

$$T - T_{ideal} = T_{ideal} \cdot \frac{\rho_0 (1 - X_A^{liq})^2}{\Delta H_A} \tag{8}$$

In Figs. 4 and 5, we illustrate the effects of ΔH_A and ρ_0 on typical liquidus curves calculated according to Eqns. 7 and 8.

In adapting the above treatment to the chlorophyll *a*/DSPC system, we ignore the partial miscibility of chlorophyll *a* and DSPC in the solid solution phase (phase II) and assume that the thermodynamic properties of the DSPC in this solid solution to be sufficiently similar to those for a pure DSPC solid. Since the solubility of chlorophyll *a* in solid DSPC is small, the error introduced by this assumption can be shown to be quite unimportant. Secondly, in as much as we are dealing with a compound type of diagram, we consider the end compositions as those of the end phases. In the present case these are pure DSPC or 0.0 mole

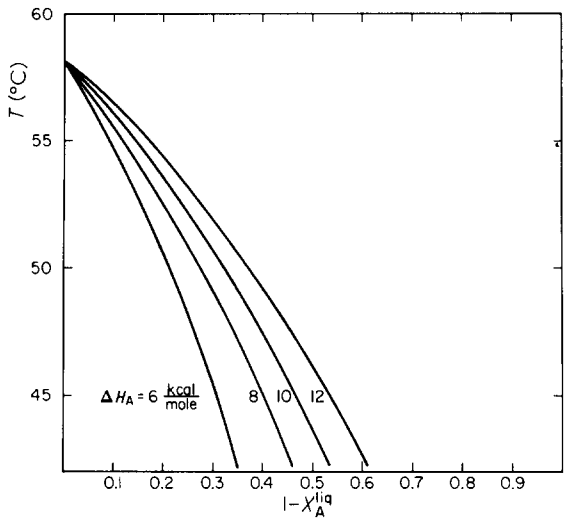

Fig. 4. Effect of ΔH_A on theoretical liquidus curves calculated according to Eqn. 7 assuming ideal solution phase mixing and a T_A of 58°C.

fraction chlorophyll *a*, and the compound phase or 0.40 mole fraction chlorophyll *a*. Thus in the simulation of the chlorophyll *a*/DSPC phase diagram, we vary X_A^{liq} between 1.00 and 0.00 as the chlorophyll *a* composition is varied between 0.00 and 0.40, i.e. we scale the value of $1 - X_A^{liq}$ by 2.5 so that $1 - X_A^{liq} =$

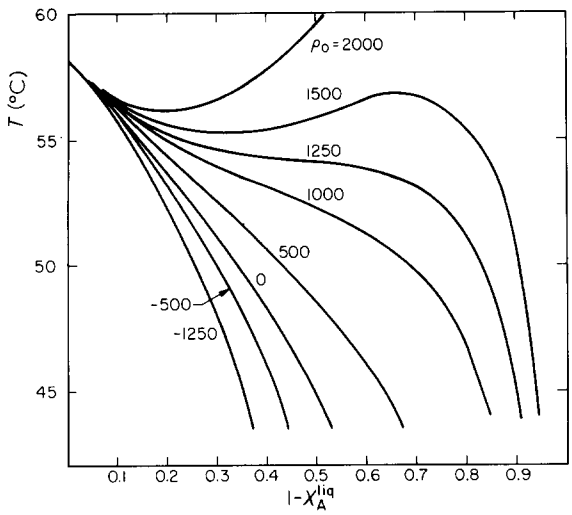

Fig. 5. Theoretical liquidus curves for nonideal solution phase mixing calculated according to Eqn. 7 and 8. Parameters: ΔH_A = 10 840 cal/mol; T_A = 58°C; ρ_0 as indicated.

TABLE I

THERMODYNAMIC VALUES OBTAINED BY SIMULATION OF THE PHASE DIAGRAM LIQUIDUS CURVES

	ΔH_A (cal/mol)	T_A (°C)	ρ_0 (cal/mol)
Liquidus left of eutectic (X_B = 0.00 to X_B = 0.32) [a]	10 840	59.5	1 180
Liquidus right of eutectic (X_B = 0.32 to X_B = 0.40) [a]	45 000	55.2	−10 000

[a] B ≡ chlorophyll *a*.

2.5 ($X_{chlorophyll}$) for the left-hand liquidus. Similarly, the liquidus right of the eutectic can be calculated using $1 - X_A^{liq} = 2.5\,(0.40 - X_{chlorophyll})$.

We have varied systematically the parameters ΔH_A, T_A, and $\rho_0$in Eqns. 7 and 9 to obtain the best agreement between the calculated and experimental liquidus for the chlorophyll *a*/DSPC system. Both the left and right liquidus curves were calculated with the best set of parameters determined independently for each. These parameters are summarized in Table I. Fig. 3 shows the simulated phase diagram along with the experimental differential thermal analysis data. The fit can be seen to be good, It should be noted that an acceptable fit of the data can be obtained only with the compound composition as the end-phase. Under no circumstances could the data be simulated using 100% chlorophyll *a* as the composition of the end-phase. This we take as further support for the choice of the compound phase diagram interpretation.

Significance of the phase diagram parameters

The liquidus left of the eutectic represents the solubility curve of DSPC in the chlorophyll *a*/DSPC solution. The value of the transition enthalpy for the formation of solid DSPC from chlorophyll *a*/DSPC solution agrees with corresponding values for pure DSPC multilayers [22,23], indicating that the phase transition is not influenced by the presence of chlorophyll *a*. The value obtained for the transition temperature for the pure component A or DSPC is slightly higher than published values [22,23] for pure DSPC, possibly reflecting a systematic error, due perhaps to our using the peak rather than the onset of the exotherm as the measured transition temperature.

The value determined for ρ_0, the nonideality parameter, indicates that mixing of DSPC and chlorophyll *a* in the solution phase is indeed nonideal, although not substantially different than for mixtures of other lipids [20].

The liquidus to the right of the eutectic represents the solubility of the compound phase in the chlorophyll *a*/DSPC solution. The values of T_A, ΔH_A and ρ_0 obtained in this case are therefore characteristic of the compound phase. T_A, the melting temperature (or dissociation temperature) of the pure compound phase is 55.2°C. ΔH_A, the corresponding transition enthalpy is about 45 kcal/mol compound or about 4-times the transition enthalpy of pure DSPC. The larger heat is possibly a reflection of both the heat of formation of the compound as well as the molecularity of the compound phase.

Finally, we discuss the significance of ρ_0. According to Eqn. 6, a positive value of ρ_0 corresponds to a positive excess free energy of mixing. Thus the ρ_0 of 1180 cal/mol obtained for the mixing between chlorophyll *a* and DSPC in the solution phase at low chlorophyll *a* concentration indicates that this mixing is energetically somewhat unfavorable. By contrast, the extremely large negative ρ_0 of −10000 cal/mol obtained for mixing of chlorophyll *a* and DSPC in the region of the compound phase indicates that the mixing is extremely favorable under these conditions. The latter result most certainly reflects the strong tendency towards compound formation in this concentration range and suggests a well defined chemical interaction between chloropyll *a* and DSPC when the stoichiometric conditions are favorable.

Conclusions

The phase diagram obtained for the chlorophyll *a*/DSPC multilamellar system suggests a number of significant conclusions regarding the properties of chlorophyll *a* in a phospholipid bilayer matrix: (1) Its phase behavior, or in other words it organization and intermolecular interactions, can be much different depending on the temperature and composition of the system. (2) Phase separation can occur within the membrane over certain temperature ranges resulting in an inhomogeneous system. (3) Chlorophyll *a* can interact with phospholipids to give a compound phase of defined stoichiometry.

It is clear from this work that the normal phase behavior of a membrane can be altered by the inclusion of chlorophyll *a*. This effect can be pronounced at high chlorophyll compositions, although for very low chlorophyll concentrations the bulk phases are not substantially different from those of the pure-lipid membrane. Thus chlorophyll *a* can be used as a nonperturbing probe of the properties of the membrane as, for example, in the fluorescence studies of Lee [11], but only when used in very small amounts. At chlorophyll *a* compositions of more than a few mole percent, however, the membrane begins to acquire a character which reflects the influence of chlorophyll *a*.

Depending on temperature and composition, the phase state of the membrane and the organization of chlorophyll *a* can vary substantially. Consider the phase changes with temperature of three different compositions of DSPC and chlorophyll *a* as an illustration. At low chlorophyll *a* concentrations, say 4 mol%, chlorophyll *a* is in a liquid solution phase of DSPC above 58°C, phase-separated into liquid solution and solid solution DSPC/chlorophyll *a* phases between 56–58°C and in a solid solution exclusively below 56°C. At medium chlorophyll *a* concentrations, say 20 mol%, chlorophyll *a* is again in a solution phase above 55°C and phase-separated into liquid solution and solid solution phases between 50–55°C, but forms a compound phase below 50°C. At even higher chlorophyll *a* compositions, above about 32 mol%, compound is formed at all temperatures below the liquidus and is the predominant chlorophyll-containing phase below 50°C. In interpreting the physical and spectroscopic properties of chlorophyll *a* in a bilayer membrane, it is therefore essential to consider the phase state of the membrane and the organization and environment of chlorophyll in the particular phase.

Acknowledgments

This work was supported by United States Public Health Service Grant GM-22432 and by National Research Service Award GM-07616 and GM-01262 from the National Institute of General Medical Sciences.

References

1 Mehreteab, A. and Strauss, G. (1978) Photochem. Photobiol. 28, 369–375
2 Colbow, K. (1973) Biochim. Biophys. Acta 314, 320–327
3 Tomkiewicz, M. and Corker, G.A. (1975) Photochem. Photobiol. 22, 249–256
4 Nicholls, P., West, J. and Bangham, A.D. (1974) Biochim. Biophys. Acta 363, 190–201
5 Oettmeier, W., Norris, J.R. and Katz, J.J. (1976) Z. Naturforsch. 31c, 163–168
6 Podo, F., Cain, J.E. and Blasie, J.K. (1976) Biochim. Biophys. Acta 419, 19–41
7 Colbow, K. (1973) Biochim. Biophys. Acta 318, 4–9
8 Dijkmans, H., LeBlanc, R.M., Cogniaux, F. and Aghion, J. (1979) Photochem. Photobiol. 29, 367–372
9 Oettmeier, W., Norris, J.R. and Katz, J.J. (1976) Biochem. Biophys. Res. Commun. 71, 445–451
10 Steinemann, A., Stark, G. and Läuger, P. (1972) J. Membrane Biol. 9, 177–194
11 Lee, A.G. (1975) Biochemistry 14, 4397–4402
12 Ritt. E. and Walz, D. (1976) J. Membrane Biol. 27, 41–54
13 Iriyama, K., Ogura, N. and Takamiya, A. (1974) J. Biochem. 76, 901–904
14 Strain, H.H., Thomas, M.R., Crespi, H.L., Blake, M.I. and Katz, J.J. (1960) Ann. N.Y. Acad. Sci. 84, 617–666
15 Strain, H.H., Thomas, M.R. and Katz, J.J. (1963) Biochim. Biophys. Acta 75, 306–311
16 Seely, G.R. and Jensen, R.G. (1965) Spectrochim. Acta 21, 1835–1845
17 Smyth, H.T. (1951) J. Am. Ceram. Soc. 34, 221–224
18 Gordon, P. (1968) Principles of Phase Diagram in Materials Systems, pp. 186-191, McGraw-Hill, New York
19 Lee, A.G. (1978) Biochim. Biophys. Acta 507, 433–444
20 Lee, A.G. (1977) Biochim. Biophys. Acta 472, 285–344
21 Eckert, C.A. (1976) in Solutions and Solubilities (Dack, M.R.J., ed.), Part II, Wiley, New York
22 Hinz, H.J. and Sturtevant, J.M. (1972) J. Biol. Chem. 247, 6071–6075
23 Phillips, M.C., Williams, R.M. and Chapman, D. (1969) Chem. Phys. Lipids 3, 234–244
24 Eigenberg, K.E., Croasmun, W.R. and Chan, S.I. (1982) Biochim. Biophys. Acta 679, 361–368